

Research article

THE MOLECULAR CLONING OF GLIAL FIBRILLARY ACIDIC PROTEIN IN *Gekko japonicus* AND ITS EXPRESSION CHANGES AFTER SPINAL CORD TRANSECTION

DEHONG GAO¹, YONGJUN WANG², YAN LIU², FEI DING²,
 XIAOSONG GU^{2*}, and ZHENGLI LI^{1*}

¹Department of Anatomy, Tongji Medical College of Huazhong University of Science & Technology, Wuhan, HB 430030, P.R. China, ²Jiangsu Key Laboratory of Neuroregeneration, Nantong University, 19 Qixiu Road, Nantong, JS 226007, P.R. China

Abstract: The glial fibrillary acidic protein (GFAP) is an astrocyte-specific member of the class III intermediate filament proteins. It is generally used as a specific marker of astrocytes in the central nervous system (CNS). We isolated a GFAP cDNA from the brain and spinal cord cDNA library of *Gekko japonicus*, and prepared polyclonal antibodies against gecko GFAP to provide useful tools for further immunochemistry studies. Both the real-time quantitative PCR and western blot results revealed that the expression of GFAP in the spinal cord after transection increased, reaching its maximum level after 3 days, and then gradually decreased over the rest of the 2 weeks of the experiment. Immunohistochemical analyses demonstrated that the increase in GFAP-positive labeling was restricted to the white matter rather than the gray matter. In particular, a slight increase in the number of GFAP positive star-shaped astrocytes was detected in the ventral and lateral regions of the white matter. Our results indicate that reactive astrogliosis in the gecko spinal cord took place primarily in the white matter during a short time interval, suggesting that the specific astrogliosis evaluated by GFAP expression might be advantageous in spinal cord regeneration.

Key words: Glial fibrillary acidic protein, Gecko, Regeneration, Spinal cord, Real-time PCR

*Authors for correspondence. e-mail. lizhengli123@hotmail.com (Zhengli Li) and neurongu@public.nt.js.cn (Xiaosong Gu)

Abbreviations used: GFAP – glial fibrillary acidic protein; IPTG – isopropyl-β-D-thiogalactopyranoside; RACE – rapid amplification of cDNA ends; SDS-PAGE – sodium dodecyl sulfate polyacrylamide gel electrophoresis

INTRODUCTION

Glial fibrillary acidic protein (GFAP) is the major subunit of the intermediate filaments of astroglial cells, one of the most abundant cell types in the vertebrate central nervous system (CNS). This protein is used extensively as a specific marker for astrocytes in the CNS [1, 2]. Human GFAP is a 432-amino acid long polypeptide encoded by the GFAP gene on chromosome 17q21 [3-6]. The 2.9-kb astrocytic mRNA of GFAP encodes the dominating GFAP isoform (GFAP α) in the CNS [3, 4]. Four other isoforms have been described, termed GFAP β , γ , δ and ϵ , and at least ϵ is functionally distinct [7]. GFAP is a member of the class III intermediate filament proteins, which have a characteristic structure composed of a highly conserved central α -helical rod domain flanked by non-helical N-terminal head and C-terminal tail domains [8-11].

GFAP is thought to be associated with the modulation of astrocyte motility and shape by providing structural stability to extensions of astrocytic processes. Astrocytes in the mammalian CNS perform such activities as processing neurotransmitters, controlling extracellular ion levels, regulating the direction and amount of nerve growth, maintaining the blood-brain barrier, and participating in immune reactions [12]. GFAP shows differential expression in astrocyte differentiation [13], and the up-regulation of GFAP is considered the hallmark of the gliosis following CNS injury [14, 15]. As a general marker, GFAP expression is also responsive to neurodegenerative changes [16] after mild neuronal impairments [17].

Following CNS injury in the adult mammal, astrocytes become reactive and respond in a typical manner, referred to as astrogliosis, which is characterized by a massive up-regulation of GFAP [18]. This astrogliosis leads to the formation of glial scars, which constitute a physical and biochemical barrier to axonal regeneration [19]. Genetically modified mice were used to show that although the glial scar may be a source of molecules that inhibit axon regeneration, its formation plays a critical role in limiting the extent of the injury [20-23]. The protective role of the reactive astrocytes has been established as a prominent feature of the cellular response to spinal cord injury (SCI) [22, 23].

Gekko japonicus, a member of the *Gekkonidae* family, has the ability to regenerate its tail, including the spinal cord, after tail amputation [24]. The spinal cords of adult geckos can also regenerate after transection injury (unpublished data). In mammals, radial glia become progressively reduced in number as development proceeds, and are therefore nearly undetectable in adults [25-27]. However, in lower vertebrates, radial glia elements constitute the main pattern of astroglial cell types, and true astrocytes, usually known as star-shaped astrocytes, are rare [28]. The star-shaped astrocytes are considered more evolutionarily advanced than radial glia [29]. Given the difference in number between the radial glia and star-shaped astrocytes, we assume that the distinct reactive astrocytes produced by various astroglial cell types may be involved in the regeneration of the injured CNS in lower vertebrates. To test this hypothesis,

we cloned the full-length GFAP cDNA of *Gekko japonicus*, and examined the expression pattern of gecko GFAP at the mRNA and protein levels after spinal cord transection.

MATERIAL AND METHODS

Animals

Adult geckos were provided by the laboratory animal center of Nantong University. They were fed with mealworms and water throughout the experiment, and housed in an air-conditioned room with controlled temperature (26°C) and saturated humidity. All of the experimental protocols involving the animals had been approved by the Laboratory Animal Care and Use Committee of Nantong University. We used cooling anesthesia to minimize the suffering of the animals. The spinal cords of the geckos were exposed by laminectomy and transected at the tenth lumbar vertebrae level. After surgery, the animals were returned to their cages and allowed to survive for 1, 3 or 7 days, or 2 weeks.

Molecular cloning and bioinformatic analyses of GFAP

The expressed sequence tag (EST) of the gecko *GFAP* was obtained from the brain and spinal cord cDNA library for *Gekko japonicus* [30]. Since the fragment did not contain the 5' regions of the cDNA, the 5' rapid amplification of the cDNA ends (RACE) was conducted using a commercially available kit (BD Biosciences Clontech), thus obtaining the full-length transcript of the GFAP gene. The total RNA was prepared from the brain and the spinal cord of the geckos using TRIZOL (Invitrogen) reagent according to the manufacturer's protocol. The primers designed for 5'RACE were: 5'-CTGAGGCTGGCCGTC TTCAGCTTGGTGA-3', (the gene-specific primer), and 5'-GAAGGCACAT ATCTGCGGCCGGGG-3' (the nested gene-specific primer).

Afterwards, the RACE-Ready first-strand cDNA was synthesized using the CDS primer and BD SMART II A oligo provided with the kit, and 5'RACE PCR was performed with the Universal Primer A Mix (UPM) under the following conditions: one cycle of 94°C for 3 min, five cycles of 94°C for 30 s and 72°C for 2 min, five cycles of 94°C for 30 s, 70°C for 30 s, and 72°C for 2 min, twenty-five cycles of 94°C for 30 s, 68°C for 30 s, and 72°C for 2 min, and one cycle of 72°C for 10 min. After agarose gel electrophoresis, the PCR-amplified product was gel purified and cloned into pGEM-T Easy vector (Promega), and sequenced as described. The full-length cDNA sequence was obtained by combining the fragment with the overlapped region.

The sequence of *GFAP* was analyzed for coding probability with the DNATools programs [31]. The comparison against the GenBank protein database was performed using the BLAST network server at the National Center for Biotechnology Information [32]. The molecular weight and the theoretical pI of the GFAP protein were analyzed by the ProtParam tool in ExPASy (<http://www.expasy.ch/tools/protparam.html>). A phylogenetic tree was constructed

via the neighbor-joining method within the PHYLIP 3.69 software package [33] using 1,000 bootstrap replicates.

Northern blot analysis

Digoxigenin-labeled GFAP riboprobes of about 300 bases were synthesized *in vitro* from linearized plasmid following the DIG-UTP supplier's instructions (Roche). The total RNAs were extracted with Trizol (Invitrogen) from various tissues of the geckos, including the brain, spinal cord, liver, kidneys, lungs and heart. A total of twenty micrograms of RNA from each tissue were separated by electrophoresis, blotted onto Nylon membrane (Schleicher & Schuell Bioscience Inc.), and cross-linked to the Nylon membrane via UV-light using a crosslinker (UV Crosslinker Applilinker Compact). Prehybridization was performed at 68°C for 3 h in a standard hybridization buffer containing 50% (v/v) formamide, 5 × SSC, 0.2% (w/v) SDS, and 2% (w/v) blocking reagent (Roche). The membrane was then hybridized in the same buffer with DIG-labeled GFAP riboprobes (1 µg/ml in DIG Easy Hyb) at 60°C for 16 h, and washed twice in 2 × SSC with 0.1% SDS at 25°C for 5 min each time and twice in 0.1 × SSC with 0.1% SDS at 68°C for 15 min each time. Then, the membrane was incubated in a blocking buffer (100 mM maleic acid, 150 mM NaCl and 1% blocking reagent) for 1 h at 37°C, and in a blocking buffer with anti-Digoxigenin-AP (1:5000, Roche) overnight at 4°C. After three washes with 100 mM maleic acid (pH 7.5) and 0.3% Tween-20, each for 15 min at 25°C, the membrane was incubated in a detection buffer containing 100 mM Tris-HCl (pH 9.5) with 100 mM NaCl for 5 min. The hybridized bands were visualized by CDP-Star (Roche) and recorded with x-ray film.

RNA isolation and real-time quantitative PCR

Total RNA was prepared with Trizol (Invitrogen) from a section stretching 5 mm rostral and 5 mm caudal from the injury epicenter of the spinal cord for the control and injured animals (n = 15 each) 1, 3, 7, and 14 days after SCI. Quantification was performed by measuring the absorption at 260 nm, and the 260/280 nm absorption ratio of the samples was verified as 1.9. Reverse transcription (RT) was performed using an Omniscript Reverse Transcription Kit (QIAGEN) in a 20 µl reaction system containing 2 µg total RNA, 0.2 U/µl M-MLV reverse transcriptase, 0.5 mM dNTP mix and 1 µM Oligo-dT primer. The first-strand cDNA was diluted to 1:3, and 4 µl was used in each 20-µl PCR reaction. PCR primers for gecko *GFAP* cDNA (accession: GU045301), and for gecko eukaryotic elongation factor 1 alpha (EF-1α) were designed corresponding to the coding regions: GFAP primers, sense 5'-CGACGCTTCGTTCCCAT-3' and antisense 5'-CCCCAAAGGCACCTACAAG-3'; EF-1α primers, sense 5'-GATGGAAAGTGACCCGCA-3' and antisense 5'-GAGGAAGACGCAGAGGTTTG-3'. The reaction mixtures included 10 µl of 2X Fast Evagreen qPCR Master Mix (Biotium), 2 µl of 10X ROX (Biotium), 4 µl of the forward and reverse primers, each at a final concentration of 100 nM, and 4 µl of cDNA. Real-time PCR was performed in a StepOne Real-time PCR system (ABI Applied Biosystems). The thermal cycling program consisted of 2 min at 96°C, followed

by 45 cycles of 15 sec at 96°C and 1 min at 60°C. Data collection was done during the 60°C extension step. To account for the variability in the total RNA input, the expression of GFAP was normalized to EF-1 α . In addition, a negative control without the first-strand cDNA was also performed.

Plasmid construction and expression of the fusion proteins

The full-length open reading frame (ORF) of the gGFAP (gecko GFAP) gene was PCR amplified using the primers 5'GFAPF (5'-CGGGATCCATGGAGGGCGCAA-3') and 3'GFAPR (5'-CCGCTCGAGTACACCACCTCCTTG-3'), which have BamHI and XhoI restriction sites (underlined), and digested with BamHI and XhoI. The digested 1.39-kb amplified cDNA was ligated into the digested pGEX-4T-1 vector and transformed to yield the pGEX-4T-1-gGFAP clone (in *E. coli* BL21), which could express a glutathione S-transferase-gGFAP fusion protein in bacteria and would contain the cleavage site of thrombin protease between the GST and gGFAP domains. The pGEX-4T-1-gGFAP construct was transformed into *E. coli* BL21 for subsequent expression.

A 20-ml overnight culture from a single colony of the *E. coli* BL21 transformants was grown in 1 l of LB base broth containing 50 μ g/ml of ampicillin at 37°C with shaking at 250 rpm until the optical density at 600 nm reached 0.4 to 0.5. To obtain a sufficient amount of soluble GST-gGFAP, the expression was optimized by induction using 0.1 mM isopropyl- β -D-thiogalactopyranoside (IPTG) and further expression at 16°C for 20 h with shaking at 250 rpm. The *E. coli* culture was centrifuged at 10,000 \times g for 10 min at 4°C, and the cell pellet was suspended in phosphate-buffered saline (PBS), pH 7.4, and sonicated for 90 s at 200 W on ice. The sonicate was then centrifuged at 12,000 \times g for 30 min at 4°C. The expression and solubility of GST-gGFAP were analyzed in parallel using 12% SDS-PAGE followed by staining with Coomassie brilliant blue R-250 at room temperature. The supernatant was purified by using glutathione Sepharose 4B (Amersham) according to the manufacturer's instructions. The fusion protein was prepared for the generation of anti-serum after the removal of the GST tag by Restriction-Grade Thrombin (Novagen). The concentration of protein was estimated using the BCA method (calibrated on Bovine serum albumin).⁷

Preparation of gGFAP polyclonal antibodies

Rabbits were immunized with recombinant gecko GFAP protein (200 μ g) by intramuscular injection at 7-day intervals for 4 consecutive weeks. The first dose was administered with Freund's complete adjuvant, while subsequent doses were given with Freund's incomplete adjuvant. The rabbits were bled a week after the last dose by cardiac puncture, and the antibody titers were determined by plate ELISA as described by Engvall and Perlman [34].

Western blot analysis

Samples were immediately removed from a section stretching 5 mm rostral and 5 mm caudal from the injury epicenter of the spinal cord for the control and

injured animals (n = 15 each) 1, 3, 7, and 14 days after SCI, and were lysed in lysis buffer containing 1% NP-40, 50 mmol/l Tris (pH 7.5), 5 mmol/l EDTA, 1% SDS, 1% sodium deoxycholate, 1% TritonX-100, 1 mmol/l PMSF, 10 mg/ml aprotinin and 1 mg/ml leupeptin. After centrifugation at 12,000 r/min for 20 min at 4°C, 20 µg of total protein of each sample was loaded into a 12% SDS-PAGE gel and transferred to PVDF membranes (Millipore). The membrane was then blocked with 5% non-fat dry milk in TBS containing 0.05% Tween-20 (TBS-T) for 1 h, and incubated with polyclonal anti-gGFAP rabbit IgG (1:1,000), prepared as described above, or anti-β-actin mouse IgG (1:1,000; Sigma-Aldrich). After the reaction with the second antibody, goat anti-mouse-IRDye (1:10,000) or donkey anti-rabbit-IRDye (1:10,000), the membrane was scanned with an Odyssey Infrared imager (LiCor, Lincoln, NE).

Immunohistochemistry

The control and injured animals (n = 5 each) were killed 3 days post-injury, and perfused intracardially with a fixative solution containing 4% paraformaldehyde in 0.1 mol/l phosphate buffer (pH 7.4). The spinal cords of the control and injured animals were removed and post-fixed overnight at 4°C in the same fixative, which was replaced with 20% sucrose for 2-3 days and then 30% sucrose for 2-3 days. Afterwards, the spinal cords were embedded in OTC compound. The 10-µm frozen cross-sections of the 2 mm of the spinal cord below the injury epicenter were prepared, and blocked with 10% goat serum with 0.3% TritonX-100 and 1% (w/v) bovine serum albumin (BSA) for 2 h at room temperature. They were incubated overnight at 4°C with polyclonal anti-gGFAP rabbit IgG (1:200), followed by reaction with FITC-conjugated secondary antibodies for 2 h at room temperature. The stained sections were examined with a DMR fluorescent microscope (Leica Microsystems, Wetzlar, Germany).

Statistical analysis

All of the data was expressed as means ± SD, and one-way ANOVA followed by Tukey's *post hoc* multiple comparison tests was applied using the Stata 7.0 statistics software. A difference was accepted as significant if $P < 0.05$. Each experiment consisted of at least three independent samples per protocol.

RESULTS

Molecular cloning and sequence analysis of gecko *GFAP* cDNA

The clone of gecko *GFAP* (GenBank accession number: GU045301) was based on the EST sequence from the brain and the spinal cord cDNA library of *Gekko japonicus*. A primary PCR product of 5'-RACE showed a band of about 200 bp, and a nested amplification yielded a band of about 150 bp. The positions of the gene-specific primer and nested gene-specific primer are shown in Fig. 1. The overlapped region was then joined to create the full-length cDNA (Fig. 1), and the full-length fragment was amplified successfully via PCR (data not shown).

```

ACGCGGGGATCTGTCTGAGTCCACGGAGCCCGGAGGAGAACCCTGACCATGGAGGGGGCGC 60
AAGCTGTGTCCTACGGGAAGCGCTTTGGCTCGTCAACCCACCTCCGTCCATCAGGCCCTG 120
K L S S Y G K R F G S S P T S V H Q A L 24
AGGTTCTCCCCGGCCGCAGATATGTGCCTTCAACCCACCCACCCGGTTCTCCGTCACC 180
R F S P G R R Y V P S N P T T R F S V T 44
AAGCTGAAGACGGCCAGCCTCAGCTTCCGCGCCGGCCCCAAATTCTCCCCAGACAAGGTG 240
K L K T A S L S F R A G P K F S P D K V 64
GATTTCTCCCTGGCGGACGCCCTCAACACAGAATTCAGGAGACCCGCACCAATGAGAAG 300
D F S L A D A L N T E F K E T R T N E K 84
GTGGAGATGATGGAGCTGAACGACCCGCTTCGCCAGCTACATCGAGAAGGTCGGCTTCCTG 360
V E M M E L N D R F A S Y I E K V R F L 104
GAGCAACAGAACAAGTCTTGGTCGCCGAGCTCAACCCAGATCCGGGACAAAGAGCCACG 420
E Q Q N K V L V A E L N Q I R D K E P T 124
AAGCTAGCCGACATCTACCGGAAGAGCTGCGGGAGCTGCGCCGACAGGTGGACCAAGCTC 480
K L A D I Y Q E E L R E L R R Q V D Q L 144
TCCAGTTCCAAGGCGAGGCTGGAGATCGAGCGGGACAATCTGGTGGAGGACCTCAACAA 540
S S S K A R L E I E R D N L V E D L N N 164
CTCCGGCACAAGTTACAGGACGAGATTAATCTGCGCCTGGAAGCCGAAAACAATTTGTCA 600
L R H K A L Q D E I N L R L E A E N N L 184
TCCTACAGACAGGATGTTGATGATGCTGCACTGGCCCGCACAGACCTGGAGCGGAAAAAT 660
S Y R Q D V D D A A L A R T D L E R K I 204
GAATCCCTGCAAGAGGAGATCAGCTTTTAAAGAAAGTGCATGAAGAGGAGCTGCGGGAG 720
E S L Q E E I S F L K K V H E E E L R E 224
CTGCTGGAACAGCTGCAGCAGCAGCAAGTCCACATCGAGATGGACGTGGCCAAGCCAGAC 780
L L E Q L Q Q Q Q Q V H I E M D V A K P D 244
CTGACATCGGCCCTGCGGGAGATCCGCCTCCAGTATGAGTCCATGGCTTCCAACAACATG 840
L T S A L R E I R L Q Y E S M A S N N M 264
CACGAGACCGAGGAGTGGTACAAATCCAAGTTTGCAGACCTGACTGATGCAGCAGCTCGA 900
H E T E E W Y K S K F A D L T D A A A R 284
AATATCGAAGCCCTGCGCCTGGCCAAGCAAGAAGCCAATGAGTACCGCCGGCAGCTGCAA 960
N I E A L R L A K Q E A N E Y R R Q Q L Q 304
GCCCTACCTGTGACTTGGAGTCCCTGCGAGGCTCGAATGAATCGCTGGAGAGGCGAGCTG 1020
A L T C D L E S L R G S N E S L E R Q L 324
AGAGAGATGGAAGACCGCTATGCCCATGATACAGCCAGCTACCAGGACACGATGATCCGG 1080
R E M E D R Y A H D T A S Y Q D R 344
CTGGAGGAAGACCCAGACTCTCAAGGAGGAAATGGCCC GGCACCTCCGGAGTACCAG 1140
L E E D T Q T L K E E M A R H L Q E Y Q 364
GACCTTCTGAATGTCAAGCTGGCCCTGGATGTGGAGATTGCCACCTACCGCAAGCTTCTG 1200
D L L N V K L A L D V E I A T Y R K L L 384
GAAGGAGAGGAAAGCAGGATCACCGTCCCTGTGCAGACTTTCTCCAACCTTCAGATCCGA 1260
E G E E S R I T V P V Q T F S N L Q I R 404
GAAACCGAGTCTGGACACAAAGTCTGTTTCTGAGGCCACCTGAAGAGGAGCCTAGTGGTC 1320
E T S L D T K S V S E A H L K R S L V V 424
AAAACGGTGGAGACCAGAGATGGCGAGGTGATCAAGGAGTCCACCCAGGAGCACAAGGAG 1380
K T V E T R D G E V I K E E S T Q E H K E 444
GTGGTGTGAAAGCAGCAGCCAGCGGTAGAGGAGCGCGCCTATAGCTGATGATGCTAGG 1440
V V * 446
AGAGCCGGCCTGCCTTCCGACGCTTCGTTCCCATGTCCACAAACAGCCCGGATCTGCAG 1500
CAGCTGCCCAAGTGTGCCCATGCTGGCAAGAGGCACAGAAGCATTGTCAGATCTAATCC 1560
TGCAATTCCTAAGTTGCCGTCAGGCGCTGTCGATTCAGCCTCTTGTAGGTGTCTTTGGGG 1620
GGATCTGACTCCTGACTCTTCTCCCGCCTCTTCAATTAGCCAGGTTGCTTCTCCAAC 1680
GGCGGTTTAGACGAGACCGTGGCTTGTCTAGACCTCAGAATCGGGTGCCTTCTCAATAAAC 1740
CTACTAACAAATAAAAAAAAAAAAAAAAAAAAA 1770

```

Fig. 1. The sequence of GFAP cDNA (GenBank accession number: GU045301) and its deduced amino acid sequence. The full-length cDNA of GFAP was 1,770 bp, and the open reading frame encoded a polypeptide of 446 amino acids. The in-frame stop codon is double underlined in the 5'UTR region, and the polyadenylation signal is underlined in the 3'UTR region. The primers of 5'-RACE including the nested primer are boxed. The numbering of the nucleotide and amino acid sequences is shown on the right.

The full-length cDNA of GFAP was 1,770 bp, and the longest open reading frame covered from 49 to 1,389 bp, which encoded a polypeptide of 446 amino acids. There is a polyadenylation signal (AATAAA) at 1,734 to 1,739 bp within the 3'-untranslated region (UTR), and an in-frame stop code at 16 to 18 bp within the 5'-UTR (Fig. 1).



Fig. 2. The alignment of GFAP using the MegAlign program (DNASTAR) created via the CLUSTAL method. The shaded (with solid black) residues are the amino acids that match the consensus. The most divergent region in the head domain is boxed. GFAP amino acid sequences were obtained from previously reported sequences in GenBank. *Gekko japonicus* (GU045301), *Gallus gallus* (XM_418091), *Danio rerio* (NM_131373), *Rattus norvegicus* (NM_017009), *Mus musculus* (NM_001131020), *Pongo abelii* (NM_001132319) and *Homo sapiens* (NM_002055).

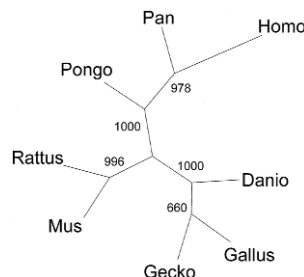


Fig. 3. A phylogenetic tree analysis of *Gekko japonicus* GFAP and other species was constructed using neighbor-joining methods within the package PHYLIP 3.69. Bootstrap majority consensus values on 1,000 replicates are indicated at each branch. The sequences obtained from GenBank are *Gekko japonicus* (GU045301), *Gallus gallus* (XM_418091), *Danio rerio* (NM_131373), *Rattus norvegicus* (NM_017009), *Mus musculus* (NM_001131020), *Pongo abelii* (NM_001132319), *Pan troglodytes* (XM_511561) and *Homo sapiens* (NM_002055).

The nucleotide sequence of gecko GFAP and its deduced amino acid sequence were analyzed using the ProtParam tool in ExPASy (<http://cn.expasy.org/>). The predicted molecular weight of the gecko GFAP protein was 52 kDa, and its theoretic pI was 5.26. The amino acid sequences of the gecko GFAP protein from different species were aligned using the CLUSTAL method in the DNASTAR software package. At the amino acid level, alignment with the human GFAP revealed 71% identity (Fig. 2). The alignment of gecko GFAP with that of other species also showed that protein divergence between species is more pronounced in the head domain (Fig. 2). The phylogenetic analysis of the GFAP of gecko and other species showed that *Gallus gallus* has the closest relationship with *Gekko japonicus* among the species selected for analysis (Fig. 3).

Tissue expression of gecko GFAP mRNA

Northern blotting was conducted to assess the size of the gecko GFAP transcript and its tissue distribution. A total of 20 µg of RNA from each tissue was analyzed in agarose formaldehyde denaturing gel, and the blot was hybridized with the DIG-labeled GFAP RNA probe. In adult geckos, GFAP expression was detectable in the brain and spinal cord, but not detectable in the liver, kidneys, lungs or heart (Fig. 4). An approximately 1.8-kb band of GFAP transcript was detected in the assay (Fig. 4), which was consistent with the full-length cDNA of GFAP as described above.

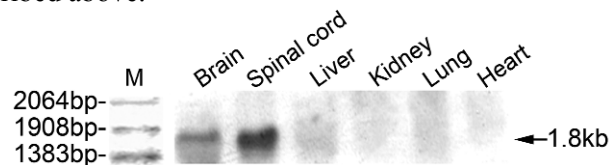


Fig. 4. The representative results of Northern blot analyses of GFAP mRNA in various tissues of the adult gecko. The bands indicate/band indicates the position of molecular size equivalent to 1.8 kb. M: RNA marker.

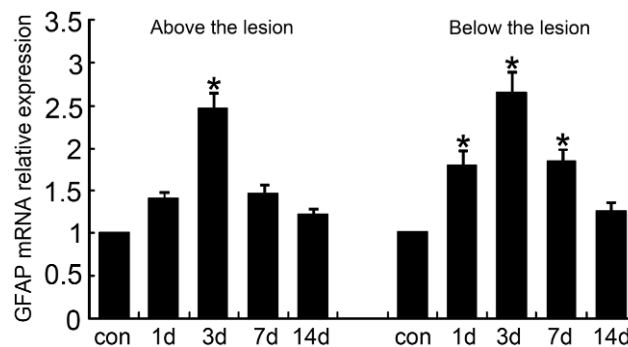


Fig. 5. Real-time qPCR analysis of GFAP expression in the spinal cord after transection. Quantitative results for RT-PCR amplification of GFAP above and below the lesion for the controls (con) and 1, 3, 7 and 14 days after spinal cord transection (n = 15 for each group). *Eukaryotic elongation factor 1 alpha (EF-1 α)* was used for the quantitative normalization. *P < 0.05.

GFAP mRNA expression after spinal cord transection in geckos

To investigate the time-dependent change in gecko *GFAP* mRNA expression after spinal cord injury (SCI), we performed real-time quantitative PCR. Total RNA was prepared from a section stretching 5 mm rostral and 5 mm caudal from the injury epicenter of the spinal cord for the control and injured animals 1, 3, 7, and 14 days after SCI. The expression of *GFAP* mRNA in the gecko spinal cord close to the injury site increased, reaching its highest level 3 days after transection, and then gradually decreased over the remainder of the 2 weeks of the experiment (Fig. 5).

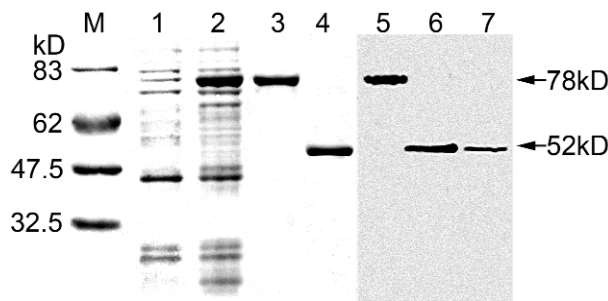


Fig. 6. Purification of gGFAP. M = protein molecular weight markers. SDS-PAGE (12%) analysis of the extracts of *Escherichia coli* BL21 before and after induction with 0.1 mM isopropyl- β -D-thiogalactopyranoside (IPTG) at 16°C (lanes 1, 2), purified GST-gGFAP from elution (lane 3) and gGFAP after Thrombin cleavage (lane 4). Western blot analysis of GST-gGFAP (lane 5), gGFAP (lane 6) and gecko brain tissues (lane 7) with polyclonal anti-gGFAP rabbit IgG.

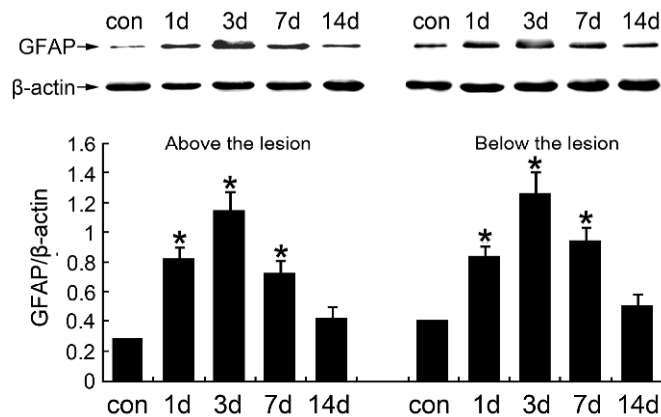


Fig. 7. Western blot analysis of GFAP expression in the spinal cord after transection. The time points selected for the experiment were the control, and 1, 3, 7, and 14 days above and below the lesion ($n = 15$ for each group) after spinal cord transection. The representative results of Western blot are shown in the upper panel, and the statistical analysis is shown in the lower panel. β -actin was used for the quantitative normalization. * $P < 0.05$.

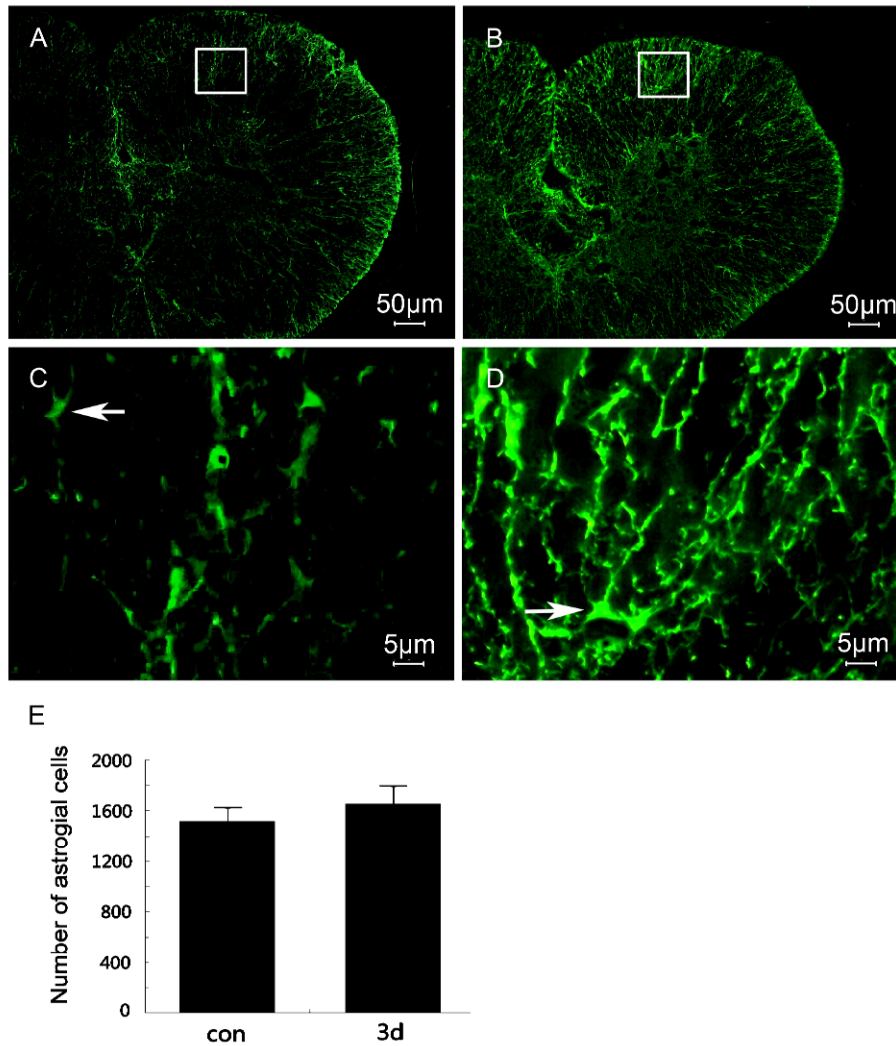


Fig. 8. GFAP immunohistochemical analysis of the adult gecko spinal cord for 2 mm caudal to the lesion in control animals (A, C) and animals 3 days after injury (B, D). $n = 5$ for each group. The white arrows show the staining of GFAP in the astrocytes. Scale bar: 50 μm (A, B) and 5 μm (C, D). Counts of astroglial cells of the gecko spinal cord 2 mm below the lesion site before (con) and 3 days after hemisection did not show any significant increase (E).

GFAP protein expression after spinal cord transection in geckos

To perform Western blot analysis and immunohistochemistry, we prepared the antibodies of gecko GFAP. The recombinant plasmid pGEX-4T-1-gGFAP was constructed and used to express the fusion protein (Fig. 6, lane 2). The prepared polyclonal anti-gGFAP rabbit IgG (Fig. 6, lanes 5 and 6) was validated

using the purified gecko GFAP protein (Fig. 6, lanes 3 and 4) via Western blot analysis, and the specificity of the antibodies was further confirmed using the brain tissue of geckos (Fig. 6, lane 7) also via Western blot analysis. The titer of the antibodies prepared via immunization with the recombinant gecko GFAP protein was measured as 1:10,000 via ELISA.

Western blot analysis was performed to determine the time-dependent change in GFAP protein expression after gecko spinal cord injury. We noted that the protein level exhibited a change trend analogous to that for the mRNA level (Fig. 7). An immunohistochemical analysis was done to determine the location of the astrocytes in the spinal cords of the geckos after SCI. In the spinal cords of the control animals, GFAP was extensively distributed in the white matter, but poorly distributed in the gray matter, except in the periependymal zone (Fig. 8A), while star-shaped astrocytes were detected mainly in the ventral regions of the white matter (Fig. 8C). By contrast, for the injured animals, an increase in the labeling of processes appeared in the white matter, especially in the ventral and lateral regions of the white matter, and ventrally at the boundary between the white and the gray matter, but few GFAP-positive star-shaped astrocytes were detected in the gray matter (Fig. 8B, D). The number of star-shaped astrocytes was not significantly increased after SCI (Fig. 8E).

DISCUSSION

It is well known that after injury to the mammalian CNS, a glial scar forms around the injury site. This glial scar is composed of reactive astrocytes extending their hypertrophied processes to form both a physical barrier, by forming an interwoven network of processes, and a chemical barrier, by releasing inhibitory factors such as chondroitin sulfate proteoglycans (CSPGs) [19]. The glial scar has traditionally been regarded as inhibitory to axon regeneration. GFAP expression was regarded as a sensitive and reliable marker labeling reactive astrocytes responding to CNS injuries [35, 36]. Other molecular markers that have been used for the immunohistochemical identification of astrocytes and reactive astrocytes include glutamine synthetase and S100 β [37, 38], but these molecules are not exclusive to astrocytes. *Gekko japonicus* has the ability to regenerate the spinal cord after transection. The process of astrogliosis following SCI in geckos is still unknown, so we aimed to use GFAP to evaluate this after SCI in geckos.

We first identified the gecko *GFAP* cDNA, encoding a 446-amino acid protein. It has a high homology with that of other vertebrates. The predicted molecular weight of the protein was 52 kDa, compared to the 50 kDa of human GFAP. The length variation of the 3'-UTR between gecko, mouse and human was observed, and this heterogeneity seemed to be due to a lack of evolutionary constraint. The 5'-UTR in mammalian *GFAP* genes is extremely short, determined to be only 15 bp long in humans and mice. A short 5'-UTR also seems to exist in the gecko *GFAP* cDNA. Analysis of the gecko GFAP amino acid sequence revealed that

the head domain contained a high number of potential serine/treonine phosphorylation sites, namely 27% of the N-terminal 60 amino acids. The phosphorylation status of the head domain has been known to be related to filament deassembly and to protein turnover [39, 40]. The amino acid sequences of the tail domain were well-conserved between humans and geckos, both having the same length. In particular, gecko GFAP showed the conserved RDG motif (residues 430-432 in gGFAP), which might be required for filament formation [41]. Northern blot analysis indicated that the *GFAP* transcript was restrictively expressed in the CNS [42].

Subsequent investigation of the astrogliosis after spinal cord transection, via detection of GFAP expression using both real-time qPCR and western blot, found that the GFAP expression level was associated with the process of SCI and regeneration in geckos. The GFAP expression increased and reached its maximum level after 3 days, and then decreased to the control level over the remainder of the 2-week experiment. Data from a mammalian CNS injury showed that mouse GFAP expression increased significantly after SCI, reaching a peak at 4 weeks and persisting for months [43-46]. The effect of reactive astrocytes in mammalian CNS after injury seems to be two-fold: reactive astrocytes play a beneficial role, such as the promotion of synaptic regeneration in the acute stage after CNS injury, but later act as inhibitors of CNS regeneration [47]. The reactive astrogliosis evaluated by GFAP expression occurs in the gecko spinal cord after transection within a short span of time, suggesting that the astrogliosis exerts non-detrimental functions in spinal cord regeneration, and possibly avoids the formation of the glial scar. However, this conclusion requires further study.

With immunohistochemical analysis, the staining of GFAP increased intensely in the white matter after spinal cord transection, but not obviously in the gray matter. In the ventral and lateral region of the white matter, a slight increase in the number of GFAP-positive star-shaped astrocytes was detected after spinal cord transection, but few could be detected in the gray matter. It has been shown that in the rat model, gray matter astrocytes have a higher potential reactivity than white matter astrocytes after SCI, as indicated by an increase in the number of labeled cells and a distinct hypertrophy [48], contributing to massive scarring in the gray matter [49, 50]. Axon regeneration is at least partially dependent on the permissivity of a glial scar [51]; blockage of astrocyte hypertrophy and hyperplasia could improve axonal regrowth, essentially in the gray matter [48, refer to discussion]. Limited reactive astrogliosis in the gray matter of the gecko spinal cord after transection might be advantageous for axon regeneration, because less reactive astrocytes render the local glial scar less capable of impeding axonal regeneration. On the basis of differences in the cellular morphologies and anatomical locations, astrocytes have usually been divided into two main subtypes, protoplasmic or fibrous astrocytes. Protoplasmic astrocytes are found throughout all gray matter, whereas fibrous astrocytes are found throughout all white matter [52]. Various lines of evidence suggest that

there is considerable molecular, structural, and potentially functional diversity of astrocytes. Our results regarding GFAP-positive astrocytes in the *Gekko japonicus* spinal cord differ from those for mammals, which are characterized by fewer star-shaped astrocytes in the ventral and lateral columns of the white matter and ventrally at the boundary between the white and the gray matters, consistent with those for the *Eublepharis macularius* spinal cord [28]. Whether the specific distribution of star-shaped astrocytes and the acute reactive astrogliosis in the white matter were involved in the spinal cord regeneration deserves further study.

To summarize, we characterized a *GFAP* cDNA from *Gekko japonicus*, and examined the tissue distribution of *GFAP*. We also detected GFAP expression changes in the gecko spinal cord close to the injury site at both the mRNA and protein levels after transection. Our results revealed that the process of gecko GFAP-positive reactive astrogliosis was different from that in mammals, which were incapable of spinal cord regeneration after SCI, suggesting that the specific reactive astrogliosis could be involved in the spinal cord regeneration.

Acknowledgements. This study was supported by the Hi-Tech Research and Development Program of China (863 Program, Grant No. 2006AA02A128), the Natural Science Foundation of Jiangsu (Grant No. BK2008010) and the Basic Research Program of the Jiangsu Education Department (09KJA180005).

REFERENCES

1. Eng, L.F., Vanderheagen, J.J., Bignami, A. and Gerstl, B. An acidic protein isolated from fibrous astrocytes. **Brain Res.** 28 (1971) 351-354.
2. Bignami, A., Eng, L.F., Dahl, D. and Uyeda, C.T. Localization of the glial fibrillary acidic protein in astrocytes by immunofluorescence. **Brain Res.** 43 (1972) 429-435.
3. Reeves, S.A., Helman, L.J., Allison, A. and Israel, M.A. Molecular cloning and primary structure of human glial fibrillary acidic protein. **Proc. Natl. Acad. Sci.** 86 (1989) 5178-5182.
4. Bongcam-Rudloff, E., Nister, M., Betsholtz, C., Wang, J.L., Stenman, G., Huebner, K., Croce, C.M. and Westermark, B. Human glial fibrillary acidic protein: complementary DNA cloning, chromosome localization, and messenger RNA expression in human glioma cell lines of various phenotypes. **Cancer Res.** 51 (1991) 1553-1560.
5. Isaacs, A., Baker, M., Wavrant-De, Vrieze, F. and Hutton, M. Determination of the gene structure of human GFAP and absence of coding region mutations associated with frontotemporal dementia with parkinsonism linked to chromosome 17. **Genomics** 51 (1998) 152-154.
6. Eng, L.F., Ghirnikar, R.S. and Lee, Y.L. Glial fibrillary acidic protein: GFAP-31 years (1969-2000). **Neurochem Res.** 25 (2000) 1439-1451.

7. Nielsen, A.L., Holm, I.E., Johansen, M., Bonven, B., Jorgensen, P. and Jorgensen, A.L. A new splice variant of glial fibrillary acidic protein, GFAP epsilon, interacts with the presenilin proteins. **J. Biol. Chem.** 277 (2002) 29983-29991.
8. Geisler, N. and Weber, K. The amino acid sequence of chicken muscle desmin provides a common structural model for intermediate filament proteins. **EMBO J.** 1 (1982) 1649-1656.
9. Steinert, P.M. and Roop, D.R. Molecular and cellular biology of intermediate filaments. **Annu. Rev. Biochem.** 57 (1988) 593-625.
10. Parry, D.A.D. and Steinert, P.M. Intermediate filament structure. **Curr. Opin. Cell Biol.** 4 (1992) 94-98.
11. Liedtke, W., Edelmann, W., Bieri, P.L., Chiu, F.C., Cowan, N.J., Kucherlapati, R. and Raine, C.S. GFAP is necessary for the integrity of CNS white matter architecture and long-term maintenance of myelination. **Neuron** 17 (1996) 607-615.
12. Kimelberg, H.K. and Norenberg, M.D. Astrocytes. **Sci. Am.** 260 (1989) 66-76.
13. Bonni, A., Sun, Y., Nadal-Vicens, M., Bhatt, A., Frank, D.A., Rozovsky, I., Stahl, N., Yancopoulos, G.D. and Greenberg, M.E. Regulation of gliogenesis in the central nervous system by the JAK-STAT signaling pathway. **Science** 278 (1997) 477-483.
14. Eng, L.F. and Ghirnikar, R.S. GFAP and astrogliosis. **Brain Pathol.** 4 (1994) 229-237.
15. Ransom, B., Behar, T. and Nedergaard, M. New roles for astrocytes (stars at last). **Trends Neurosci.** 26 (2003) 520-522.
16. May, P.C., Boggs, L.N., Fuson, K.S., Bender, M., Li, W., Miller, F.D., Hyslop, P., Calligaro, D., Seubert, P., Johnson-Wood, K., Chen, K., Games, D. and Schenk, D. GFAP as a marker of plaque pathology in PDAPP transgenic mouse. **Soc. Neurosci. Abstr.** 23 (1997) 1638.
17. Canady, K.S. and Rubel, E.W. Rapid and reversible astrocytic reaction to afferent activity blockade in chick cochlear nucleus. **J. Neurosci.** 12 (1992) 1001-1009.
18. Bignami, A. and Dahl, D. The astrocytic response to stabbing. Immunofluorescence studies with antibodies to astrocytic-specific protein (GFAP) in mammalian and submammalian vertebrates. **Neuropathol. Appl. Neurobiol.** 2 (1976) 99-110.
19. Silver, J. and Miller, J.H. Regeneration beyond the glial scar. **Nat. Rev. Neurosci.** 5 (2004) 146-156.
20. Wang, X., Messing, A. and David, S. Axonal and nonneuronal cell responses to spinal cord injury in mice lacking glial fibrillary acidic protein. **Exp. Neurol.** 148 (1997) 568-576.
21. Menet, V., Prieto, M., Privat, A. and Gimenezy, Ribotta, M. Axonal plasticity and functional recovery after spinal cord injury in mice deficient in both glial fibrillary acidic protein and vimentin genes. **Proc. Natl. Acad. Sci.** 100 (2003) 8999-9004.

22. Faulkner, J.R., Herrmann, J.E., Woo, M.J., Tansey, K.E., Doan, N.B. and Sofroniew, M.V. Reactive astrocytes protect tissue and preserve function after spinal cord injury. **J. Neurosci.** 24 (2004) 2143-2155.
23. Okada, S., Nakamura, M., Katoh, H., Miyao, T., Shimazaki, T., Ishii, K., Yamane, J., Yoshimura, A., Iwamoto, Y., Toyama, Y. and Okano, H. Conditional ablation of Stat3 or Socs3 discloses a dual role for reactive astrocytes after spinal cord injury. **Nat. Med.** 12 (2006) 829-834.
24. Cristino, L., Pica, A., Della, Corte, F. and Bentivoglio, M. Plastic changes and nitric oxide synthase induction in neurons which innervated the regenerated tail of the lizard Gekko gekko II. The response of dorsal root ganglion cells to tail amputation and regeneration. **Brain Res.** 871 (2000) 83-93.
25. Pixley, S.K. and De, Vellis, J. Transition between immature radial glia and mature astrocytes studied with a monoclonal antibody to vimentin. **Brain Res.** 317 (1984) 201-209.
26. Voigt, T. Development of glial cells in the cerebral walls of ferrets: direct tracing of their transformation from radial glia into astrocytes. **J. Comp. Neurol.** 289 (1989) 74-88.
27. Elmquist, J.K., Swanson, J.J., Sakaguchi, D.S., Ross, L.R. and Jacobson, C.D. Developmental distribution of GFAP and vimentin in the Brazilian opossum brain. **J. Comp. Neurol.** 344 (1994) 283-296.
28. Lazzari, M. and Franceschini, V. Intermediate filament immunohistochemistry of astroglial cells in the leopard gecko, *Eublepharis macularius*. **Anat. Embryol.** 210 (2005) 275-286.
29. Kalman, M. and Pritz, M.B. Glial fibrillary acidic protein-immunopositive structures in the brain of acrocodilian, *Caiman crocodilus*, and its bearing on the evolution of astroglia. **J. Comp. Neurol.** 431 (2001) 460-480.
30. Liu, Y., Ding, F., Liu, M., Jiang, M., Yang, H., Feng, X. and Gu, X. EST-based identification of genes expressed in brain and spinal cord of Gekko japonicus, a species demonstrating intrinsic capacity of spinal cord regeneration. **J. Mol. Neurosci.** 29 (2006) 21-28.
31. Rehm, B.H. Bioinformatic tools for DNA/protein sequence analysis, functional assignment of genes and protein classification. **Appl. Micro-Biol. Biotechnol.** 57 (2001) 579-592.
32. Altschul, S.F., Madden, T.L., Schaffer, A.A., Zhang, J., Zhang, Z., Miller, W. and Lipman, D.J. Gapped BLAST and PSI-BLAST: a new generation of protein database search programs. **Nucleic Acids Res.** 25 (1997) 3389-3402.
33. Felsenstein, J. PHYLIP (phylogeny inference package). version 3.6. Department of Genome Sciences, University of Washington, Seattle (2004).
34. Engvall, E. and Perlman, P. Enzyme-linked immunosorbent assay (ELISA). Quantitative assay of immunoglobulin G. **Immunochemistry** 8 (1971) 871-874.
35. Rataboul, P., Faucon, Biguet, N., Vernier, P., De, Vitry, F., Boularand, S., Privat, A. and Mallet, J. Identification of a human glial fibrillary acidic

- protein cDNA: a tool for the molecular analysis of reactive gliosis in the mammalian central nervous system. **J. Neurosci. Res.** 20 (1988) 165-175.
36. Hozumi, I., Chiu, F.C. and Norton, W.T. Biochemical and immunocytochemical changes in glial fibrillary protein after stab wounds. **Brain Res.** 524 (1990) 64-71.
 37. Goncalves, C.A., Leite, M.C. and Nardin, P. Biological and methodological features of the measurement of S100B, a putative marker of brain injury. **Clin. Biochem.** 41 (2008) 755-763.
 38. Norenberg, M.D. Distribution of glutamine synthetase in the rat central nervous system. **J. Histochem. Cytochem.** 27 (1979) 756-762.
 39. Inagaki, K., Gonda, T., Nishizawa, K., Kitamura, S., Sato, C., Ando, S., Tanabe, K., Kikuchi, K., Tsuiki, S. and Nishi, Y. Phosphorylation sites linked to glial filament disassembly in vitro locate in a non-alpha-helical head domain. **J. Biol. Chem.** 265 (1990) 4722-4729.
 40. Takemura, M., Gomi, H., Colucci-Guyon, E. and Itohara, S. Protective role of phosphorylation in turnover of glial fibrillary acidic protein in mice. **J. Neurosci.** 22 (2002) 6972-6979.
 41. Chen, W.J. and Liem, R.K. The endless story of the glial fibrillary acidic protein. **J. Cell Sci.** 107 (1994) 2299-2311.
 42. Bock, E. Nervous system specific proteins. **J. Neurochem.** 30 (1978) 7-14.
 43. Nestic, O., Lee, J., Johnson, K.M., Ye, Z., Xu, G.Y., Unabia, G.C., Wood, T.G., McAdoo, D.J., Westlund, K.N., Hulsebosch, C.E. and Regino, Perez-Polo, J. Transcriptional profiling of spinal cord injury-induced central neuropathic pain. **J. Neurochem.** 95 (2005) 998-1014.
 44. Tian, D.S., Dong, Q., Pan, D.J., He, Y., Yu, Z.Y., Xie, M.J. and Wang, W. Attenuation of astrogliosis by suppressing of microglial proliferation with the cell cycle inhibitor olomoucine in rat spinal cord injury model. **Brain Res.** 1154 (2007) 206-214.
 45. Ritz, M.F. and Hausmann, O.N. Effect of 17beta-estradiol on functional outcome, release of cytokines, astrocyte reactivity and inflammatory spreading after spinal cord injury in male rats. **Brain Res.** 1203 (2008) 177-188.
 46. Huang, X., Kim, J.M., Kong, T.H., Park, S.R., Ha, Y., Kim, M.H., Park, H., Yoon, S.H., Park, H.C., Park, J.O., Min, B.H. and Choi, B.H. GM-CSF inhibits glial scar formation and shows long-term protective effect after spinal cord injury. **J. Neurol. Sci.** 277 (2009) 87-97.
 47. Pekny, M., Wilhelmsson, U., Bogestål, Y.R. and Pekna, M. The role of astrocytes and complement system in neural plasticity. **Int. Rev. Neurobiol.** 82 (2007) 95-111.
 48. Morin-Richaud, C., Feldblum, S. and Privat, A. Astrocytes and oligodendrocytes reactions after a total section of the rat spinal cord. **Brain Res.** 783 (1998) 85-101.
 49. Collins, G.H. and West, N.R. Glial activity during axonal regrowth following cryogenic injury of rat spinal cord. **Brain Res. Bull.** 22 (1989) 71-79.

50. Soriede, A.J. Variations in the perineural glial changes after different types of nerve lesion: light and electron microscopic investigations on the facial nucleus of the rat. **Neuropathol. Appl. Neurobiol.** 7 (1981) 195-204.
51. Alonso, G. and Privat, A. Reactive astrocytes involved in the formation of lesional scars differ in the mediobasal hypothalamus and in other forebrain regions. **J. Neurosci. Res.** 34 (1993) 510-522.
52. Sofroniew, M.V. and Vinters, H.V. Astrocytes: biology and pathology. **Acta Neuropathol.** 119 (2010) 7-35.